Accepted Manuscript



Multi-isotopic tracing (Mo, S, Pb, Re—Os) and genesis of the Mo—W Azegour skarn deposit (High-Atlas, Morocco)

Éric Marcoux, Noémie Breillat, Catherine Guerrot, Philippe Négrel, Samia Berrada Hmima, David Selby

PII: S1464-343X(19)30114-1

DOI: https://doi.org/10.1016/j.jafrearsci.2019.04.007

Reference: AES 3481

To appear in: *Journal of African Earth Sciences*

Received Date: 21 November 2018

Revised Date: 8 April 2019

Accepted Date: 8 April 2019

Please cite this article as: Marcoux, É., Breillat, Noé., Guerrot, C., Négrel, P., Hmima, S.B., Selby, D., Multi-isotopic tracing (Mo, S, Pb, Re—Os) and genesis of the Mo—W Azegour skarn deposit (High-Atlas, Morocco), *Journal of African Earth Sciences* (2019), doi: https://doi.org/10.1016/j.jafrearsci.2019.04.007.

This is a PDF file of an unedited manuscript that has been accepted for publication. As a service to our customers we are providing this early version of the manuscript. The manuscript will undergo copyediting, typesetting, and review of the resulting proof before it is published in its final form. Please note that during the production process errors may be discovered which could affect the content, and all legal disclaimers that apply to the journal pertain.

ACCEPTED MANUSCRIPT

Multi-isotopic tracing (Mo, S, Pb, Re-Os) and genesis of the Mo-W Azegour skarn deposit (High-Atlas, Morocco)

2019, February 25th

Éric Marcoux (1), Noémie Breillat (2), Catherine Guerrot (3), Philippe Négrel (4), Samia Berrada Hmima (5), David Selby (6)

(1) Corresponding author
University of Orléans, ISTO, UMR 7327, 45071, Orléans, France
eric.marcoux@univ-orleans.fr

(1), (2), (3) and (4) - BRGM, ISTO, UMR 7327, BP 36009, 45060 Orléans, France - CNRS/INSU, ISTO, UMR 7327, 45071 Orléans, France - University of Orléans, ISTO, UMR 7327, 45071, Orléans, France
(5) - Laboratoire Géo-Ressources, URAC 42, Département de Géologie, Faculté des Sciences et Techniques de Marrakech, Université Cadi Ayyad, Marrakech, Morocco
(6) - Department of Earth Sciences, Durham University, Durham DH1 3LE, UK - State Key Laboratory of Geological Processes and Mineral Resources, School of Earth Resources, China University of Geosciences, Wuhan, China

Regular Article submitted to Journal of African Earth Sciences – Revised version

Abstract

The Mo-Cu-W Azegour skarn, located in the High-Atlas in Morocco, is associated with a Late Hercynian alkaline granitic intrusion. Here the origin of the mineralisation via Re-Os geochronology and using Mo, S and Pb isotopes is discussed. The age of mineralization defined by Re-Os molybdenite geochronology is 276 ± 1.2 Ma for the Azegour mine, and 267 ± 1.2 for the Tizgui deposit suggesting for multiple mineralization events associated with the Hercynian alkaline granitic intrusion. The $\delta^{98}Mo_{NIST}$ of molybdenite range from -0.60 ‰ to 0.42 ‰ (n=26) for the Azegour mine and from 0.08 ‰ to 0.40 ‰ (n=2) for the Tizgui mine. Variations of the $\delta^{98}Mo_{NIST}$ occur either at the deposit scale with a difference of about 0.72 ‰, and at the sample scale (few cm), which exhibits a difference of up to 0.40 ‰. A multi-phased mineralization is proposed as the main processes explaining the variation in the $\delta^{98}Mo_{NIST}$ values although the influence of a Rayleigh fractionation process cannot be precluded. The high $\delta^{34}S$ values determined from molybdenite, pyrrhotite, and chalcopyrite (8 to 14.7 ‰) suggest a sedimentary origin for sulphur from the Cambrian sedimentary country rocks. Whereas, the initial $^{206}Pb/^{204}Pb$ compositions of common lead (18.08 to 18.30) for

chalcopyrite and pyrrhotite imply a strong contribution of lead from the host volcano-sedimentary units.

Keywords: Azegour skarn, molybdenite, molybdenum, lead, sulphur, isotopes, Re-Os geochronology, mineralization

1. Introduction

Skarns are among the most common types of deposit in the world and have been widely studied. They form large deposits of tungsten, lead-zinc, copper and gold, and also yield tin in the form of cassiterite, and very seldomly, molybdenum.

The present study focuses on the Azegour Mo-skarn in Morocco. Located in the High-Atlas, the Azegour site (Fig. 1) is a Mo-W-Cu skarn with production from three historic mines: main Azegour, by far the main one, Tizgui and Entifa. This skarn was exploited from 1932 to 1959 supplying 1300 t of MoS_2. The Mo content is estimated around 8000 t (Permingeat, 1957). A re-opening of the mine is possible. Molybdenite is not the only economically important mineral in the Azegour skarn, scheelite and chalcopyrite were reported at economic grades (Permingeat, 1957). The existence of Mo mineralization and deposits in this area occurs over more than 3.5 km (Fig. 2).

Figure 1: Location of the Azegour skarn in North part of Moroccan High-Atlas

Molybdenum (Mo) isotopes are commonly used to investigate (paleo-)redox conditions, Mo input into the oceans from weathering, and more recently, as with other transition-meta isotopesl, for studying trace-metal pollution (Archer and Vance, 2008). In the frame of mineral resources, only few studies have been performed regarding Mo isotopes in molybdenite. These studies have principally focused on molybdenite in pegmatite veins (Greber et al., 2011), and porphyry systems (Greber et al., 2014; Shafiei et al., 2015) and on

other molybdenite-bearing ore deposits (Hannah et al., 2007; Mathur et al., 2010; Breillat et al., 2016). These studies suggest that the influence of the crystallisation temperature, stage of crystallisation, Rayleigh processes and crystal structure (2H or 3R polytypes) are factors that control the Mo isotopic composition.

Here we utilize Mo, together with Pb and S isotope data of sulphides and gangue minerals and Re-Os molybdenite geochronology to provide an improved understanding of the genesis of the Mo mineralisation of the Azegour skarn deposit system.

2. Geological context

The molybdenum-copper Azegour skarn in Morocco is located 60 km south of Marrakech in the northern boundary of High Atlas Mountains (Fig. 1) (coordinates: 31°09'16" N, 8°18'19" W). Numerous studies have discussed the geology of the Azegour skarn over the past 80 years (e.g., Moret, 1931; Heim, 1934; Permingeat, 1957; El Amrani, 1984 and Berrada et al., 2011, 2015). The skarn formed as the result of the intrusion of a Permian granite into a series of volcano- sedimentary units (Fig. 2 and 3) dated Cambrian by the presence of Archoeocyathydes (Neltner, 1938).

Figure 2: Geological map of the Azegour region. Figure 2 is fully contained in the red triangle on figure 1

The volcano-sedimentary series are composed of grey to black shales, a volcanic unit (with dominant andesitic flows and dacitic pyroclastic rocks), marbles, recrystallized limestone and dolostone. A Late Hercynian alkaline granitic intrusion (Lagarde, 1987; Mrini et al., 1992), named the Azegour granite, outcrops for 7 km along a NW-SE direction with a 1 km width. The skarn is developed within the Palaeozoic volcano-sedimentary units (Fig. 2).

Figure 3: Granite and skarn contact in Azegour

The Azegour granite is hyperaluminous (Lagarde, 1987; Ait Ayad et al., 2000) and is mainly composed of quartz, feldspar (orthoclase and plagioclase), and minor biotite. The granite crystallisation is dated at 269 ± 11 Ma (Charlot et al., 1967) and 271 ± 3 Ma (Mrini, 1985) by the Rb-Sr method. The Sr and Nd initial ratios (I_{Sr} = 0.7051; $\varepsilon_{Nd(T)}$ = -1; T = 270 Ma) obtained on the Azegour granite suggest a composite origin (crust-mantle) with a strong mantle component (Mrini, 1985; Mrini et al., 1992). Metasomatized carbonate layers constituting the skarn are several meters thick, and are mainly composed of massive garnetite and/or wollastonite-rich rock, with rare pyroxenite. Garnets belong to three different types: a green-black garnet is very common, forming crystals up to 8 cm, and composed of andradite with locally a core of Al-rich andradite (up to 5 % Al_2O_3); a very common brown-black garnet forms thick layers associated with quartz and commonly reveals a core of pure andradite surrounded by a Al-rich andradite (up to 10 % Al_2O_3), close to a grossular type, and an orange garnet (Toulkine village zone) that is compose of only grossular garnet. The abundance of spessartine is always low (4 % maximum). Wollastonite is slighly manganiferous, whereas vesuvianite is F- and Cl-rich (up to 3.3 % and 1.2 %, respectively). The mineralogical assemblage suggests the formation of the prograde stage of the skarn occurred at around 620 - 650 °C, under a pressure of 1.7 - 2 kbar, and a fCO_2 of 31 mole %, in a reducing environment (fO_2 of 10^{-18} to 10^{-16} atm.), preceding a retrograde stage. Sulphides formed during the retrograde stage (< 450 °C) (Berrada et al., 2015). The garnetites are the main Mo-bearing rocks in the form of large (up to 3 cm) molybdenite crystals (Fig. 4). Similar to molybdenite, scheelite occurs only in garnetite, whereas chalcopyrite and pyrrhotite (Fig. 5) are mainly associated with pyroxenite. The skarn is widely overlain by Cretaceous formations.

Figure 4: Coarse molybdenite (white and grey) within garnetite from the Azegour mine. Photograph in reflected light

Figure 5: Chalcopyrite (C, yellow) and pyrrhotite (Po, light brown) from Azegour mine. Photograph in reflected light

3. Methodology

3.1. Molybdenum isotopic composition

The analyses of molybdenum isotopic composition have been performed at BRGM (France) on 29 samples of molybdenite. The procedure for analysing the Mo isotopic composition in molybdenite has been described in detail in Breillat et al. (2016). As Mo is the major cation in molybdenite (59.94 %), no chemical purification prior to analysis was undertaken (Anbar et al., 2001; Barling et al., 2001; Malinovsky et al., 2007; Mathur et al., 2010). Mathur et al. (2010) evaluated possible matrix effects induced by the lack of chemical purification for molybdenite by analysing the same sample with or without purification and both results were in agreement. Around 100 mg of molybdenite (single grain for large crystals, multiple grains for disseminated molybdenite) was handpicked and then finely crushed in order to homogenize the sample. Around 10 mg of molybdenite powder were dissolved in 4 ml of *aqua regia* (1 ml of HNO_3 7N and 3 ml of HCl 8N) at 100 °C in PTFE beakers until complete dissolution. The solutions were dried and the residues were dissolved in 10 ml of HNO_3 3 % (v/v). From this concentrated solution, a final solution was prepared in HNO_3 3 % in order to get a final Mo concentration of 1 $\mu g.ml^{-1}$ (allowing a signal of around 2.5 V on mass ^{95}Mo). Zirconium was added to this solution to yield a concentration of 0.5 $\mu g.ml^{-1}$ (allowing a signal of around 4 V on mass ^{90}Zr). The Mo blank level for the whole procedure is less than 0.05 % and thus negligible as compared to the sample concentration.

The Mo-isotopic composition analyses were performed using an MC-ICP-MS Neptune (Thermo-Finnigan). Zirconium (Zr) and ruthenium (Ru) produce several isobaric interferences on 92, 94, 96 and 96, 98, 100 masses, and only ^{95}Mo and ^{97}Mo are free of interference. Such interference is easily corrected with the following cup configuration: ^{90}Zr-L3, ^{91}Zr-L2, ^{92}Mo-^{92}Zr-L1, ^{94}Mo-^{94}Zr-Ax, ^{95}Mo-H1, ^{97}Mo-H2, ^{98}Mo-^{98}Ru-H3, ^{99}Ru-H4. In our samples and standards, ruthenium has never been detected. The Mo-isotope measurements were run within sequences composed of blank, standard and sample analyses. After the sample and standard analyses, two minute washes (HNO_3 3 %) are done to get the low background values (less than 5 mV). The reported data represent the mean value of a minimum of 5 runs of 20 measurements. Mass bias was corrected by ^{90}Zr/^{91}Zr external spiking (Zirconium ICP standard CertiPUR Merck) at 0.5 µg.ml^{-1} (Anbar et al., 2001) and standard-sample-standard bracketing. The external long-term reproducibility obtained during the course of this study was 0.08 ‰ (2σ, n = 137) for an ICP standard solution (Techlab n°B3015042). In order to test the reproducibility of our procedure on the same matrix, a Re-Os molybdenite standard (Henderson Molybdenite Reference Material 8599 [RM8599], Markey et al., 2007) has been repeatedly analysed as a secondary standard. All data are reported as classic $\delta^{98}Mo_{NIST}$ units relative to a standard solution, in this case NIST SRM 3134 (lot # 891307), according to the following formula (Eq. 1):

$$\delta^{98}Mo_{NIST} = \left[\frac{(^{98}Mo/^{95}Mo)sample}{(^{98}Mo/^{95}Mo)standard} - 1\right] * 1000 \qquad \text{(Eq. 1)}$$

The NIST SRM 3134 solution (lot#891307) has been proposed as a reference for reporting Mo-isotopic compositions (Wen et al., 2010; Greber et al., 2012; Goldberg et al., 2013). Following Goldberg et al. (2013), the $\delta^{98}Mo_{NIST}$ of NIST SRM 3134 is defined as 0 ‰ and data are reported according to this value. The reference material 8599 yielded a $\delta^{98}Mo_{NIST}$ of -

0.20 ± 0.08 ‰ (2σ, n = 85; Breillat et al., 2016). Variation between samples is expressed as $\Delta^{98}Mo$ which corresponds to the difference between the maximum and the minimum values of $\delta^{98}Mo_{NIST}$.

3.2. Sulphur isotopic composition

The sulphur isotopic compositions were measured in BRGM (France) for molybdenite, chalcopyrite and pyrrhotite samples from the Azegour skarn. Molybdenite flakes were handpicked, and then crushed in agate bowl. Chalcopyrite and pyrrhotite were collected using a Dremel™ drill. Around 100 to 150 µg of the obtained powder with pentoxide of vanadium as catalyser were placed into a tin capsule. Analyses were performed on Elementary Analyser IRMS Delta V Plus (Thermo Finnigan). Sulphides were converted to SO_2 with a flash combustion at 1 000 °C and analysed after chromatographic separation. At least two replicates were performed. All data are reported as classic $\delta^{34}S_{vCDT}$ units relative to vCDT standard according to the following formula (Eq. 2):

$$\delta^{34}S_{vCDT} = \left[\frac{(^{34}S/^{32}S)sample}{(^{34}S/^{32}S)standard} - 1\right] * 1000 \quad \text{(Eq. 2)}$$

3.3. Lead isotopic composition

Lead isotopic compositions of molybdenite, chalcopyrite, pyrrhotite samples from the Azegour skarn and K-feldspar from the Azegour granite have been measured in BRGM (France) according to techniques adapted from Marcoux (1987) and Pomiès et al. (1998). After cleaning, sulphides (50 to 100 mg) are dissolved with a mixture of HNO_3 7N – HCl 6N and a drop of concentrated HBr in a Teflon container. Feldspars (200 mg) were dissolved in a closed container by using a HF-HNO_3-$HClO_4$ mixture at 120 °C for one week. After evaporation, the residue was dissolved by using HCl 6N, and heat again at 120 °C for one

week. After complete dissolution (sulphides and feldspars), the solutions were dried and then dissolved with 3-4 ml of HBr 1N. The Pb was separated on quartz columns filled with 1 ml AG1X8 ion exchange resin by using HBr and HCl acids. The lead fraction is then purified on a small 0.1 ml column by using HCl. After evaporation the residue was then recollected with HNO_3 and dried again. Blanks for the overall procedure are lower than 100 pg and are negligible relative to the amount of sample analyzed. Measurements of the lead ratios ($^{206}Pb/^{204}Pb$, $^{207}Pb/^{204}Pb$ and $^{208}Pb/^{204}Pb$) were obtained on static mode on a multicollector MAT262 Thermal Ionisation Mass Spectrometer. Samples and standards were loaded on a zone-refined Re filament previously outgassed. Silica gel was used as an emission stabilizer. About 150 ng of lead were loaded with H_3PO_4 onto each filament. The Pb isotopic ratios were corrected for a mass bias of 0.14 % per amu (atomic mass unit) determined by repeated measurements of the NBS982 standard. Individual error on all ratios is commonly better than 0.01% ($2\sigma_m$), whereas external reproducibility (2σ) is 0.06 % for the $^{206}Pb/^{204}Pb$, 0.09 % for the $^{207}Pb/^{204}Pb$ and 0.12 % for the $^{208}Pb/^{204}Pb$.

For chalcopyrite, pyrrhotite, molybdenite and K-feldspar, Pb, U and Th contents of the sample were used for correcting the measured Pb isotope ratios for the addition of radiogenic Pb, assuming a mean age of 270 ± 10 Ma. These corrections are insignificant for most of the samples due to very low U/Pb and Th/Pb values, except for AZT1a pyrrhotite ($^{238}U/^{204}Pb$ = 15.7). However, the corrected ratios for this sample are in the range of the other sulphides. For molybdenite (Mo4, Mo7, Mo8; $^{238}U/^{204}Pb$ = 0.1, 5.9 and 11.4 respectively) corrected values remain more radiogenic than the other sulphides.

3.4. Re-Os isotopic composition

198 The Re-Os analyses were performed on 3 samples of molybdenites. Samples were prepared
199 in BRGM (Orléans, France), with the chemical and mass spectrometry protocols performed
200 at Durham University (UK) in the Laboratory for sulphide and source rock geochronology and
201 geochemistry and the Arthur Holmes Laboratory, members of the Durham Geochemistry
202 Centre. Molybdenite separates of the 125 – 250 μm fraction were obtained by traditional
203 methods (crushing, heavy liquids, magnetic separator and handpicking under a microscope
204 to remove impurities).

205 The procedure for the Re-Os analyses is described in detail in Selby and Creaser (2001a, b).
206 The Carius tube method (Shirey and Walker, 1995) was used for dissolution of the
207 molybdenite and equilibration with the tracer solution (^{185}Re + normal Os). Osmium was
208 separated and purified by $CHCl_3$ solvent extraction and micro-distillation. The rhenium was
209 separated and purified using NaOH-acetone solvent extraction and anion chromatography.
210 The purified Re and Os fractions were loaded onto Ni and Pt wire filaments, respectively, and
211 analysed for their isotope composition by negative thermal ionisation mass spectrometry
212 (NTIMS) of a Triton Scientific mass spectrometer. Molybdenites have naturally high Re
213 content and no initial Os (Morgan et al., 1968; Markey et al., 1998), all the ^{187}Os is derived
214 from the decay of ^{187}Re (Faure, 1986). Model Re-Os ages were calculated using the equation
215 $\ln(^{187}Os/^{187}Re + 1)/\lambda$, using the decay constant (λ) of $1.666e^{-11}a^{-1}$ (Smoliar et al., 1996).
216 Uncertainties include all sources of analytical uncertainty (Re and Os mass spectrometer
217 measurements, blank abundances and isotopic compositions (Re = 3.2 ppt; Os = 0.3 ppt;
218 $^{187}Os/^{188}Os = 0.223 \pm 0.03$, n=1), spike calibrations and reproducibility of standard Re and Os
219 isotopic values), and with and without the uncertainty in the decay constant (0.35 %; Smoliar
220 et al., 1996; Selby et al., 2007).

4. Results

4.1. Re-Os

The results of Re-Os analyses on molybdenites are given in Table 1. The Re and ^{187}Os concentration for Tizgui MoS_2 are respectively 14.00 ± 0.05 ppm and 39.35 ± 0.13 ppb. The Re concentration for the two Azegour MoS_2 is 7.00 ± 0.03 ppm and 2.87 ± 0.01 ppb and the ^{187}Os concentration is 20.31 ± 0.07 ppb and 8.33 ± 0.02 ppb.

Table 1: Re-Os data and model dates for molybdenites analyzed in this study.

The Re-Os model age for the Tizgui mine sample is 267.79 ± 1.45 Ma, whereas the Re-Os ages for the Azegour mine are almost 10 Ma older (276.56 ± 1.51 Ma and 276.84 ± 1.49 Ma; Table 1).

4.2. Molybdenum

The molybdenite from Azegour skarn display $\delta^{98}Mo_{NIST}$ values that range between -0.60 ‰ and +0.42 ‰ (Fig. 6 and Table 2) resulting in a variation of $\Delta^{98}Mo$= 1.02 ‰. Such a variation at the scale of a deposit is coherent with the variations for other occurrences or deposits shown by previous studies. For example, Mathur et al. (2010) found a $\Delta^{98}Mo$ of around 0.75 ‰ for El Teniente ore deposit in Chile. A slightly larger variation was shown by Greber et al. (2011) for the Grimsel Pass pegmatite ($\Delta^{98}Mo$ of ~1.14 ‰) and for the Alpjahorn pegmatite $\Delta^{98}Mo$ of ~1.35 ‰). Greber et al. (2014) found a $\Delta^{98}Mo$= 0.88 ‰ in the Questa porphyry Mo ore deposit (New Mexico, USA). Additionally, Shafiei et al. (2015) reported the largest variation ($\Delta^{98}Mo$ of around 1.94 ‰) for the Kerman porphyry deposit (Iran).

Figure 6: Histogram of Mo isotopic composition of molybdenite samples from Azegour mine and Tizgui mine

The mean $\delta^{98}Mo_{NIST}$ value for the molybdenite samples of the Azegour skarn is -0.01±0.56 ‰ (2σ, n=29). This value fully agrees with the mean value of molybdenites analysed in all literature and normalized to NIST 3134 as summarized by Breillat et al. (2016) (0.04 ‰±1.04 ‰, 2σ, n=391).

We investigated the possible variation of the $\delta^{98}Mo_{NIST}$ of the Azegour skarn by analysing two samples collected in the Tizgui mine, located 2 km to the North of the Azegour mine. The molybdenite crystals of the two sites show distinct differences: massive and centimetre in size (up to 5 cm) in the Azegour mine, disseminated and millimetre in size (maximum 7 mm) in the Tizgui mine. The $\delta^{98}Mo_{NIST}$ values are 0.08 ‰ and 0.40 ‰ in the samples from the Tizgui mine, whereas the values for the Azegour mine are between -0.60 ‰ and +0.42 ‰ (Table 2). The variation within individual samples from -0.17±0.11 ‰ to 0.42±0.13 ‰ (Mo076, Table 2), giving a $\Delta^{98}Mo$ of around 0.59 ‰, is similar to the whole variation measured in the Tizgui mine and not significantly different to variations measured in this study.

Greber et al. (2011) and Shafiei et al. (2015) found evidence of multi-modality in the distribution of the $\delta^{98}Mo_{NIST}$ in molybdenites. On the contrary, in the Azegour skarn, the distribution of the data follows a Gaussian (normal) distribution, but nonetheless there is no clear evidence of multi-modality in the distribution of the $\delta^{98}Mo_{NIST}$ in the molybdenites as illustrated in the Figure 6. Given that the multi-modality is typically interpreted as representing different phases of crystallisation, the Gaussian (normal) distribution may

suggest that only one phase of crystallisation has occurred, what is clearly not the case in the Azegour skarn.

Table 2: Mo-isotope data of molybdenites analyzed for this study. Data are relative to NIST3134 ($\delta^{98}Mo_{NIST}$=0). N = number of analyses for each sample. Long-term external reproducibility of 0.08 ‰ (2σ) on $\delta^{98}Mo_{NIST}$. References to sub samples are indicated by an additional subscript a to d, meaning up to 4 subsamples, i.e. same rock sample referred MoXXX and up to 4 samples of molybdenite grain in the samples MoXXX.

4.3. Sulphur

The molybdenites from the Azegour skarn have $\delta^{34}S_{vCDT}$ values ranging between 12.4 and 14.7 ‰ and the molybdenite samples collected in the Tizgui mine exhibit nominally lower values (12.4 ‰, n=2) than those of the Azegour mine (12.7-14.7 ‰, n=27) (Table 3 and Fig. 7).

The $\delta^{34}S_{vCDT}$ values of chalcopyrite range between 10.5 and 12.5 ‰ (n=5). The $\delta^{34}S_{vCDT}$ for the pyrrhotites from Tizgui mine are 8.0 and 8.3 ‰ (n=2), with the pyrrhotites from Azegour mine possessing values of 12.2 and 14.2 ‰.

Figure 7: Histogram of $\delta^{34}S_{vCDT}$ isotopic composition of molybdenite, chalcopyrite and pyrrhotite samples

Table 3: Sulphur isotope data of molybdenites, chalcopyrites and pyrrhotites analyzed in this study.

4.4. Lead

Initial lead isotopic compositions ($^{206}Pb/^{204}Pb$, $^{207}Pb/^{204}Pb$ and $^{208}Pb/^{204}Pb$) calculated using a mean age of 270 ± 10 Ma are reported in Table 4 and Figure 8. The range of the initial lead isotope composition can be illustrated by the $^{206}Pb/^{204}Pb_i$ value, ranging for chalcopyrite, pyrrhotite and feldspar samples from 18.08 to 18.30. Chalcopyrite $^{206}Pb/^{204}Pb_i$ values are close (18.13 to 18.23), whereas pyrrhotite $^{206}Pb/^{204}Pb_i$ values exhibit a wider range from 18.08 to 18.30. The $^{206}Pb/^{204}Pb_i$ values for molybdenite are more radiogenic, between 18.51 and 20.01.

Figure 8: Pb-Pb diagrams of initial composition of chalcopyrite, pyrrhotite, and K-feldspar from Azegour granite (Mrini, 1985), with the Stacey-Kramers (1975) growth curve (SK) and Doe-Zartman (1979) orogen curve. The measured ratios have been corrected for the addition of radiogenic Pb, assuming an age of 270 Ma. Molybdenite corrected ratios are too radiogenic and do not appear on this figure. Lead isotopic composition of neighbouring ore deposits are mentioned for comparison: galena from Amensif ore deposit (Ilmen et al., 2014) and from Draa Sfar and Hajar huge VMS (Marcoux et al., 2008).

Table 4: Lead isotope data of molybdenite, chalcopyrite, pyrrhotite and K-feldspar analyzed in this study. Measured values have been corrected to an age of 270 Ma.

5. Discussion

5.1. Re-Os dating of the molybdenites

The results are consistent with the age of the granite crystallisation dated at 269 ± 11 Ma (Rb-Sr, Charlot et al., 1967) and 271 ± 3 Ma (Rb-Sr, Mrini, 1985). Therefore, we conclude that the Mo mineralisation is contemporaneous with crystallisation of the Azegour granite. However, a difference of a few million years can be observed between the molybdenite sample from Tizgui (youngest) and samples from Azegour (oldest). Molybdenite records the timing of mineralisation and by inference the age of the associated granite suggesting in this

case a multi-phased granitic intrusion. Such a magmatic-hydrothermal multi-phased history is very common in porphyry and related-skarn ore deposits (Sillitoe, 2010) as well as in major skarn deposits like Los Santos, Spain (Timon-Sanchez et al., 2009) and Salau, France (Poitrenaud et al., in press) where two successive intrusions emplaced at 269 ± 6 and 280 ± 6 Ma (K/Ar dates), and 289.1 ± 1.9 Ma and 295 ± 2 Ma (LA-ICP-MS-U-Pb dates) respectively. At Azegour we assume that the intrusion could also be multiple phased but of similar lithology or, more likely, the presence of a younger intrusion at depth that gave way to the Tizgui mineralization.

5.2. Possible causes of Molybdenum isotopic composition variations

Four processes are described in the literature to explain these variations at deposit scale and even at sample scale. First, Klemm et al. (2008) suggested that the fractionation of the Mo isotopes is due to the different stages of mineralisation, a progressive enrichment in heavy Mo isotopes in the residual melt of subvolcanic magma chamber being the cause of the variation in the Mo isotopes. The second process was described by Greber et al. (2014), which argued for a fractionation of the Mo isotopes at the magmatic-hydrothermal transition. A third process was first described by Hannah et al. (2007) and later by Klemm et al. (2008), who suggested that fractionation that occurs during the same stage of mineralisation, but also within an individual hand specimen, is due to a Rayleigh fractionation of a hydrothermal fluid and a fractionation due to fluid phase separation (brine and vapour). We recall that Rayleigh fractionation describes the evolution of a multi-phased system, an hydrothermal system in this study, in which one phase is continuously removed from the system through fractional distillation. This fractional distillation is one of the most common cause of isotopic fractionation. Finally the last process was evoked by Shafiei et al.

(2015). They suggested that the fractionation of the Mo isotopes could be controlled by the molybdenite structures (2H or 3R polytypes). When considering the whole variation of the Mo isotopes observed in our data set, the variation within individual hand samples, the lack of evidence of different values between the two sampling sites in Azegour and the two different facies, we argue that the principal process of Mo fractionation in the Azegour skarn is the succession of two phases of crystallisation evidenced by Re-Os molybdenite ages, without precluding a probable influence of Rayleigh fractionation in the hydrothermal fluid.

5.3. Source of ore-forming fluids: Sulphur isotopic composition

The high values observed mostly within molybdenite for the Azegour skarn require a contribution from a ^{34}S-enriched sulphur source. Magmatic sulphides in uncontaminated felsic magmas generally have a signature value of 0 ± 3 ‰ (Ohmoto, 1972; Hoef, 1997), in agreement with Liu et al. (2014) that suggested that $\delta^{34}S$ of between 2 and 4 ‰ indicate a magmatic sulphur source. Values for Cu-porphyry deposits are mostly between -5 ‰ and +5 ‰, with carbonate-hosted Pb-Zn ore deposits values from -20 ‰ and +20 ‰. Most skarns have $\delta^{34}S$ values between -5 ‰ and +5 ‰ (e.g. Ault and Williams-Jones, 2004) indicating a magmatic source for sulphur.

The high $\delta^{34}S$ values measured in Azegour fall outside the field values indicating a predominantly magmatic origin of sulphur in skarn deposits. The Azegour skarn is not the only skarn with high values of $\delta^{34}S$. Ishihara et al. (2000; 2002) observed a range from 11.1 ‰ to 14.8 ‰ for Geumseong molybdenum skarn deposits (Korea) and suggest that extraction and migration of sulphur of the host carbonates into the skarn mineralization. Rose et al. (1985) reported values from 6.3 to 19.9 ‰ for the Cornwall skarn (Pennsylvania, USA). These high values of $\delta^{34}S$ are well explained by a sedimentary source of sulphur and, in

some cases, a marine sedimentary source or evaporites with high $\delta^{34}S$ of sulphur cannot be precluded (e.g., Faure and Brathwaite, 2006). The Azegour skarn occurs in carbonate series with black shales from the lower Cambrian (Neltner, 1938), which usually possess a $\delta^{34}S > 20$ ‰ (Jébrak and Marcoux, 2015), and are thus likely the dominant source of sulphur for the skarn, but, given to the $\delta^{34}S$ values, a complementary source of sulphur, probably magmatic, is also required.

5.4. Source of ore-forming fluids: Lead isotopic composition

These high values indicate the influence of a more radiogenic component in their genesis. Uranium is very scarce and disseminated as tiny uraninite crystals, but Permingeat (1957) noted that, at the mine scale, uranium is preferentially associated with molybdenite but none uraninite inclusion has been observed in molybdenite. However, as initial lead isotopic compositions calculated for molybdenite are still more radiogenic than for other sulphides, explanations could be that Pb from molybdenite is sources in the more radiogenic host rocks, while Pb from other sulphides is sourced in the magmatic intrusion, what is supported by sulphur isotopic results.

Ilmen et al. (2014) have performed Pb isotopic analyses on a galena from the Amensif deposit, which is located 5 km in the south of Azegour skarn and is spatially associated with the Azegour granite. The $^{206}Pb/^{204}Pb$ isotopic values of galena (18.05, Fig. 8), close to initial isotopic values measured on Azegour sulphides, suggest that the Pb was sourced from the Lower Paleozoic volcano-sedimentary units (Ilmen et al., 2014).

Our data (molybdenite not included) define a narrower range with a mean $^{206}Pb/^{204}Pb$ value at 18.18 ± 0.07 (σ). The initial $^{206}Pb/^{204}Pb$ value of the skarn is around 18.08 - 18.30. Feldspar sample from the Azegour granite having a $^{206}Pb/^{204}Pb$ value of 18.20,

suggests that the granite cannot be considered as a major source for lead in the skarn, although its role as an accessory source cannot be discarded.

6. Summary of the origin of the ore-forming elements in Azegour

The Re-Os analyses of molybdenite (~267 and 276 Ma) provide a robust geochronology for the mineralisation of the Azegour skarn, which are broadly contemporaneous with the previous emplacement history of the granite (Rb-Sr ages determined on the granite ranging from 269 ± 11 to 271 ± 3 Ma). Although presently there is no evidence of multi-staged emplacement of the Azegour granite, the Re-Os molybdenite dates do imply two phases of mineralisation within the Azegour system, and thus the presence of a hidden younger intrusion at depth. Multi-phased crystallisation is proposed as the principal process of Mo fractionation in the Azegour skarn and could explain Mo isotopic variation in occurrence and sample scale, whereas a Rayleigh fractionation in hydrothermal fluid cannot be precluded. The ^{34}S-enrichment of the sulphide ores of the Azegour skarn suggests a strong participation of surrounding rocks. Regarding lead isotopes, the location of all Azegour samples below the Stacey and Kramers (1975) and just below Doe and Zartman (1979) orogen curves suggest that the ore forming materials are derived from a mixture of upper crustal material with an important contribution of mantle lead, a result in accordance with the previous Sr and Nd isotopic studies (Mrini, 1985).

Acknowledgments

This work is part of Noémie Breillat PhD research supported by the Region Centre and the Carnot-BRGM Institute. We thank Anne-Marie Desaulty, Anne-Marie Gallas, Anne-Thérèse Montech, Alexandre Vrain, Antonia Hoffman, Chris Ottley and Geoff Nowell for their support during laboratory work Rebecca Neely is thanked for her constructive remarks.

402 **References**

403 Ait Ayad, N., Ribeiro, M.L., Sola, A.R., Moreira, M.E., Dias, R., Bouabdelli, M., Ezzouhaira, H.,
404 Charif, A., 2000. Le Granite d'Azegour (Maroc) : cartographie géochimique et
405 interprétation géodynamique. Comunicações do Instituto Geológico e Mineiro 87,
406 155-164.

407 Anbar, A.D., Knab, K.A., Barling, J., 2001. Precise determination of mass-dependent
408 variations in the isotopic composition of molybdenum using MC-ICP-MS. Analytical
409 Chemistry 73, 1425-1431, DOI: 10.1021/ac000829w.

410 Archer, C., Vance, D. 2008. The isotopic signature of the global riverine molybdenum flux and
411 anoxia in the ancient oceans. Nature geoscience, Vol 1, 597-600.

412 Ault, K.M., Williams-Jones, A.E., 2004. Sulfur and lead isotope study of the EL Mochito Zn-Pb-
413 Ag deposit. Economic Geology, 99, 1223-1231.

414 Barling, J., Arnold, G.L., Anbar, A.D., 2001. Natural mass-dependent variations in the isotopic
415 composition of molybdenum. Earth and Planetary Science Letters 193, 447-457.

416 Berrada, S.H., Hajjaji, M., Belkabir, A., 2011. Mineralogical and geochemical features of the
417 wollastonite deposit of Azegour, Haut-Atlas (Morocco). Journal of African Earth
418 Sciences 60, 247-252, DOI: 10.1016/j.jafrearsci.2011.03.008.

419 Berrada Hmima, S., Marcoux, É., Hafid, A., 2015. Le skarn Mo-W-Cu à grenat, wollastonite,
420 pyroxène et vésuvianite d'Azegour (Haut-Atlas, Maroc). Bulletin de la Société
421 Géologique France, 186 (1), 21-34, DOI: 10.2113/gssgfbull.186.1.21.

Breillat, N., Guerrot, C., Marcoux, É., Négrel, Ph., 2016. A new global database of δ^{98}Mo in molybdenites: A literature review and new data. Journal of Geochemical Exploration, 161 : 1-15.DOI: 10.1016/j.gexplo.2015.07.019,

Charlot, R., Tisserant, D., Vidal, P., Vidal, F., 1967. Rapport technique et quelques résultats. Compte Rendu d'Activité, Service Géologique, Maroc, 126-137.

Doe, B.R., Zartman, R.E., 1979. Plumbotectonics, the Phanerozoic. Geochemistry of hydrothermal ore deposits, 22-70.

El Amrani, E.H.I., 1984. Contribution à l'étude pétrologique, minéralogique, métallogénique et de pétrologie structurale des formations de la région d'Azegour (Haut-Atlas occidental, Maroc). Thèse Doctorat 3ème cycle. Faculté des Sciences, Nancy I. France.

Faure, K., Brathwaite, R.L., 2006. Mineralogical and stable isotope studies of gold-arsenic mineralisation in the Sams Creek peralkaline porphyritic granite, South Island, New Zealand. Mineralium Deposita, 40, 802-827.

Faure, G., 1986. Principles of isotope geology. New York, John Wiley and Sons, 589p.

Goldberg, T., Gordon, G., Izon, G., Archer, C., Pearce, C.R., McManus, J., Anbar, A.D., Rehkämper, M., 2013. Resolution of inter-laboratory discrepancies in Mo isotope data: an intercalibration. Journal of Analytical Atomic Spectrometry 28, 724-735, DOI: 10.1039/C3JA30375F.

Greber, N.D., Hofmann, B.A., Voegelin, A.R., Villa, I.M., Nägler, T.F., 2011. Mo isotope composition in Mo-rich high- and low-T hydrothermal systems from the Swiss Alps. Geochimica et Cosmochimica Acta 75, 6600-6609, DOI: 10.1016/j.gca.2011.08.034.

443 Greber, N.D., Pettke, T., Nägler T.F., 2014. Magmatic–hydrothermal molybdenum isotope
444 fractionation and its relevance to the igneous crustal signature. Lithos 190-191, 104-
445 110, DOI: 10.1016/j.lithos.2013.11.006.

446 Greber, N.D., Siebert, C., Nägler, T.F., Pettke, T., 2012. $\delta^{98/95}$Mo values and molybdenum
447 concentration data for NIST SRM 610, 612 and 3134: Towards a common protocol for
448 reporting Mo data. Geostandards and Geoanalytical Research 36-3, 291-300, DOI:
449 10.1111/j.1751-908X.2012.00160.x.

450 Hannah, J.L., Stein, H.J., Wieser, M.E., de Laeter, J.R., Varner, M.D., 2007. Molybdenum
451 isotope variations in molybdenite: Vapor transport and Rayleigh fractionation of Mo.
452 Geology 35, 703-706, DOI: 10.1130/G23538A.1.

453 Heim, A., 1934. The molybdenum mine at Azegour, Morocco, Society of Economic
454 Geologists, Inc. 29, 76-83.

455 Hoefs, J., 1997. Stable Isotope Geochemistry. 4th edition. Springer-Verlag, Berlin, 1-201.

456 Ilmen, S., Alansari, A., Bajddi, A., Ennaciri, A., Maacha, L., 2014. Mineralogical and
457 geochemical characteristics of the Amensif Cu, Pb, Zn, (Ag, Au) ore deposit, Western
458 High Atlas, Morocco. Journal of Tethys 2, 118-136.

459 Ishihara, S., Jin, M.S., Sasaki, A., 2000. Source diversity of ore sulfur from Mesozoic- Cenozoic
460 mineral deposits in the Korean Peninsula region. Resource Geology 50, 203-212.

461 Ishihara, S., Kajiwara, Y., Jin, M.S., 2002. Possible carbonate origin of ore sulfur from
462 Geumseong Mo deposit, South Koera. Resource Geology 52, 279-282.

463 Jébrak M., Marcoux É., 2015. Geology of Mineral Resources. Éditions Ministère de l'Énergie
464 et des Ressources Naturelles Canada, 662 p.

465 Klemm, L.M., Pettke, T., Heinrich, C.A., 2008. Fluid and source magma evolution of the
466 Questa porphyry Mo deposit, New Mexico, USA. Mineralium Deposita 43, 533-252.

467 Lagarde, J.L., 1987. Granites tardi-carbonifères et déformation crustale. L'exemple de la
468 Meseta marocaine. Mémoires et Documents du CAES, Rennes, vol. 26 (1989) 342 p.

469 Liu, J., Mao, J.W., Wu, G., Wang, F., Luo, D.F., Hu, Y.Q., Li, T.G., 2014. Fluid inclusions and H-
470 O-S-Pb isotope systematics of the Chalukou giant porphyry Mo deposit, Heilongjiang
471 Province, China. Ore Geology Reviews, 59, 83-96

472 Malinovsky, D., Hammarlund, D., Ilyashuk, B., Martinsson, O., Gelting, J., 2007. Variations in
473 the isotopic composition of molybdenum in freshwater lake systems. Chemical
474 Geology 236, 181-198, DOI: 10.1016/j.chemgeo.2006.09.006.

475 Marcoux, É., 1987. Isotopes du plomb et paragenèses métalliques, traceurs de l'histoire des
476 gîtes minéraux. Illustration des concepts de source, d'héritage et de régionalisme
477 dans les gîtes français. Applications en recherche minière. Documents du BRGM,
478 N°117, 388p.

479 Marcoux, É., Belkabir, A., Gibson, H., Lentz, D., 2008. Draa Sfar: a Hercynian pyrrhotite–Zn–
480 Cu–Pb ore deposit in the Jebilet, Morocco. Mineralogy, geochemistry and
481 deformation as constrains for a genetic model features. Ore Geology Reviews 33,
482 307–328

483

484 Markey, R., Stein, H., Morgan, J., 1998. Highly precise Re–Os dating for molybdenite using
485 alkaline fusion and NTIMS. Talanta 45, 935-946.

486 Markey, R., Stein, H.J., Hannah, J.L., Zimmerman, A., Selby, D., Creaser, R.A., 2007.
487 Standardizing Re–Os geochronology: A new molybdenite reference material
488 (Henderson, USA) and the stoichiometry of Os salts. Chemical Geology 244, 74-87,
489 DOI: 10.1016/j.chemgeo.2007.06.002.

490 Mathur, R., Brantley, S., Anbar, A., Munizaga, F., Maksaev, V., Newberry, R., Vervoort, J.,
491 Hart, G., 2010. Variation of Mo isotopes from molybdenite in high-temperature
492 hydrothermal ore deposits. Mineralium Deposita 45, 43-50, DOI: 10.1007/s00126-
493 009-0257-z.

494 Moret, L., 1931. Recherches géologiques dans l'Atlas de Marrakech. Notes et Mémoires.
495 Service des Mines et Carte Géologique du Maroc, 18.

496 Morgan, J.W., Lovering, J.F., Ford, R.J., 1968. Rhenium and non-radiogenic osmium in
497 Australian molybdenites and other sulphide minerals by neutron activation analysis.
498 Geological Society of Australia 15, 189-194.

499 Mrini, Z., 1985. Age et origine des granitoïdes hercyniens du Maroc; Apport de la
500 géochronologie et de la géochimie isotopique (Sr, Nd, Pb). Thèse Université
501 Clermont-Ferrand, 156p.

502 Mrini, Z., Rafi, A., Duthou, J.L., Vidal, P., 1992. Chronologie Rb-Sr des granitoïdes hercyniens
503 du Maroc : conséquences. Bulletin de la Société Géologique de France 163, 281-291.

504 Neltner, L., 1938. Granites du Haut-Atlas. C.R. sommaire Société Géologique de France, 70-
505 71.

506 Ohmoto, H., 1972. Systematics of sulfur and carbon isotopes in hydrothermal ore deposits.
507 Economic Geology 67, 551–578.

508 Permingeat, F., 1957. Le gisement de molybdène, tungstène et cuivre d'Azegour (Haut Atlas)
509 : Etude pétrographique et métallogénique. Notes et Mémoires SGM 141, PhD thesis,
510 284p.

511 Poitrenaud, T., Poujol, M., Augier R., Marcoux É. – *in press*- The multi-stage story of a late-
512 Variscan W/Au deposit (Salau, French Pyrenees): Insights from REE and U/Pb LA-ICP-
513 MS analyses. Mineralium Deposita

514 Pomiès, C., Cocherie, A., Guerrot, C., Marcoux, É., Lancelot, J.R., 1998. Assessment of the
515 precision and accuracy of lead-isotope ratios measured by TIMS for geochemical
516 applications: example of massive sulphide deposits (Rio Tinto, Spain). Chemical
517 Geology, 144: 137-149.

518 Rose, A.W., Herrick, D.C., Deines, P., 1985. An Oxygen and Sulfur Isotope Study of Skarn-Type
519 Magnetite Deposits of the Cornwall Type, Southeastern Pennsylvania. Economic
520 Geology 80, 418-443.

521 Selby, D., Creaser, R.A., 2001a. Re-Os geochronology and systematics in molybdenite from
522 the Endako porphyry molybdenum de- posit, British Columbia, Canada. Economic
523 Geology 96, 197-204.

524 Selby, D., Creaser, R.A., 2001b. Late and Mid Cretaceous mineralization in the Northern
525 Cordillera: Constraints from Re-Os molybdenite dates. Economic Geology 96, 1461-
526 1467.

527 Selby, D., Creaser, R.A., Stein, H.J., Markey, R.J., Hannah, J.L., 2007. Assessment of the ^{187}Re
528 decay constant by cross calibration of Re–Os molybdenite and U–Pb zircon
529 chronometers in magmatic ore systems. Geochimica et Cosmochimica Acta 71, 1999-
530 2013.

531 Shafiei, B., Shamanian, G., Mathur, R., Mirnejad, H., 2015. Mo isotope fractionation during
532 hydrothermal evolution of porphyry Cu systems. Mineralium Deposita 50, 281-291,
533 DOI: 10.1007/s00126-014-0537-0.

534 Shirey, S.B., Walker, R.J., 1995. Carius tube digestion for low- blank rhenium-osmium
535 analysis. Analytical Chemistry 67, 2136-2141.

536 Sillitoe, R., 2010. Porphyry copper systems. Economic Geology, 105, 3-41.

537 Smoliar, M.I., Walker, R.J., Morgan, J.W., 1996. Re-Os ages of group IIA, IIIA, IVA, and IVB
538 iron meteorites. Science 271, 1099-1102.

539 Stacey, J.S., Kramers, J.D., 1975. Approximation of Terrestrial Lead Isotope Evolution by a 2-
540 Stage Model. Earth and Planetary Science Letters 26, 207-221.

541 Timon-Sanchez, S.M., Moro Benito, M.C., Cembranos Perez, M.L., 2009. Mineralogical and
542 physiochemical evolution of the Los Santos scheelite skarn, Salamanca, NW Spain.
543 Economic Geology, 104, 961-995

544 Wen, H., Carignan, J., Cloquet, C., Zhu, X., Zhang, Y., 2010. Isotopic delta values of
545 molybdenum standard reference and prepared solutions measured by MC-ICP-MS:
546 Proposition for delta zero and secondary references. Journal of Analytical Atomic
547 Spectrometry 25, 716-721, DOI: 10.1039/B921060A.

ACCEPTED MANUSCRIPT

Sample	Location	wt(g)	Re(ppm)	±	^{187}Re(ppm)
Mo78	Tizgui mine	0.021	14.00	0.05	8.80
Mo86b	Azegour mine	0.020	7.00	0.03	4.40
Mo89b	Azegour mine	0.100	2.87	0.01	1.80

*uncertainty includes that associated with the decay constant

ACCEPTED MANUSCRIPT

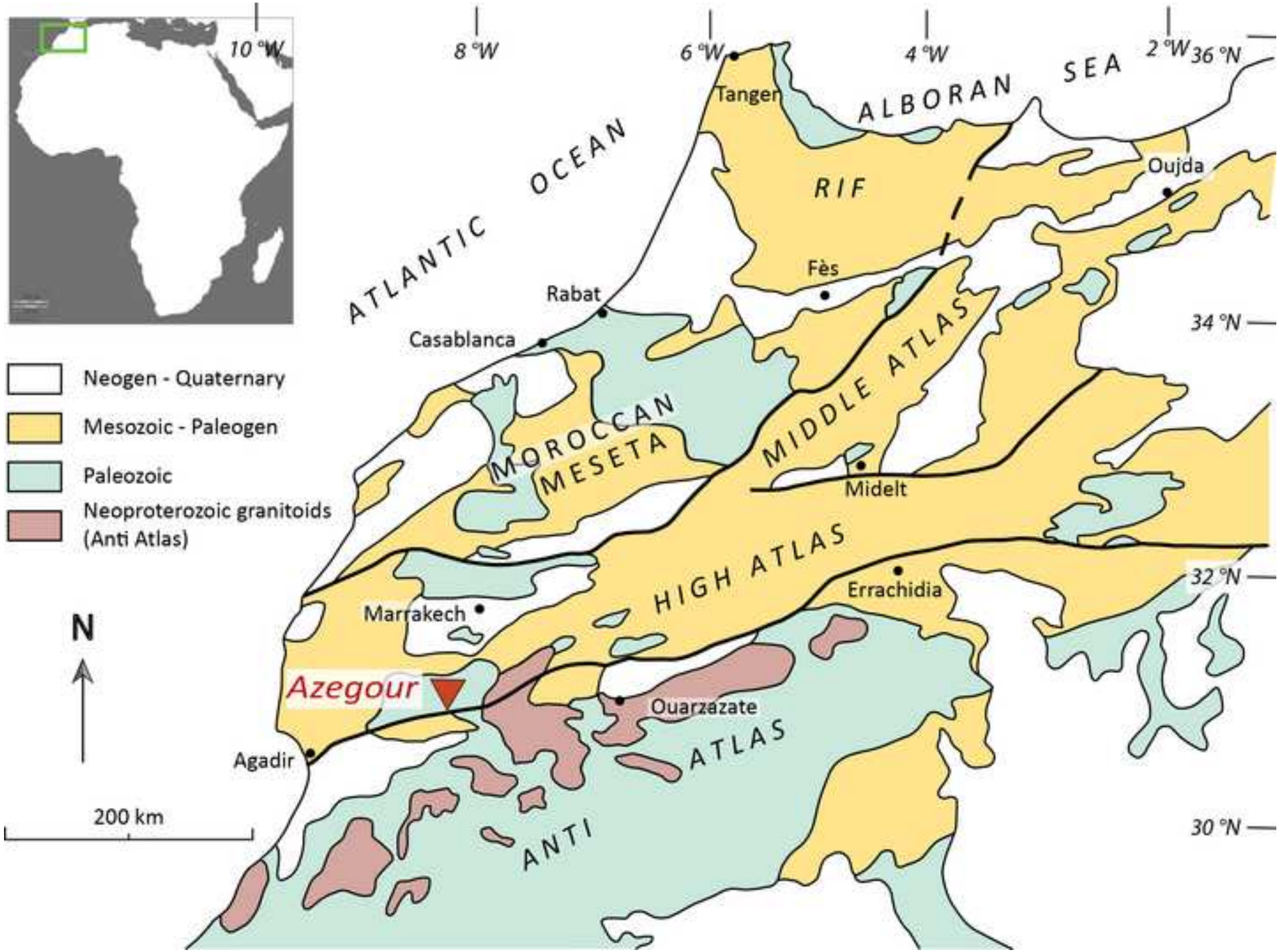
ID	Location	n	$\delta^{97}Mo_{NIST}$	2σ
Mo004	Azegour mine	6	0.05	0.09
Mo007	Azegour mine	6	-0.29	0.08
Mo008	Azegour mine	6	0.21	0.05
Mo072	Azegour mine	5	-0.35	0.06
Mo073	Azegour mine	6	-0.40	0.09
Mo074a	Azegour mine	5	0.21	0.07
Mo074b	Azegour mine	5	-0.08	0.03
Mo074c	Azegour mine	6	-0.02	0.05
Mo075a	Azegour mine	6	0.13	0.09
Mo075b	Azegour mine	6	0.23	0.07
Mo076a	Azegour mine	6	-0.08	0.07
Mo076b	Azegour mine	6	0.32	0.07
Mo077	Tizgui mine	6	0.30	0.07
Mo078	Tizgui mine	6	0.08	0.10
Mo084a	Azegour mine	5	-0.18	0.04
Mo084b	Azegour mine	5	-0.09	0.02
Mo084c	Azegour mine	5	-0.20	0.02
Mo085a	Azegour mine	5	-0.09	0.09
Mo085b	Azegour mine	5	0.02	0.08
Mo085c	Azegour mine	5	-0.14	0.04
Mo085d	Azegour mine	5	-0.08	0.03
Mo086a	Azegour mine	8	-0.13	0.09
Mo086b	Azegour mine	5	-0.18	0.07
Mo087	Azegour mine	5	0.18	0.06
Mo088a	Azegour mine	5	0.03	0.05
Mo088b	Azegour mine	5	0.17	0.07
Mo089a	Azegour mine	5	0.03	0.07
Mo089b	Azegour mine	5	0.27	0.04
Mo090	Azegour mine	5	0.11	0.04

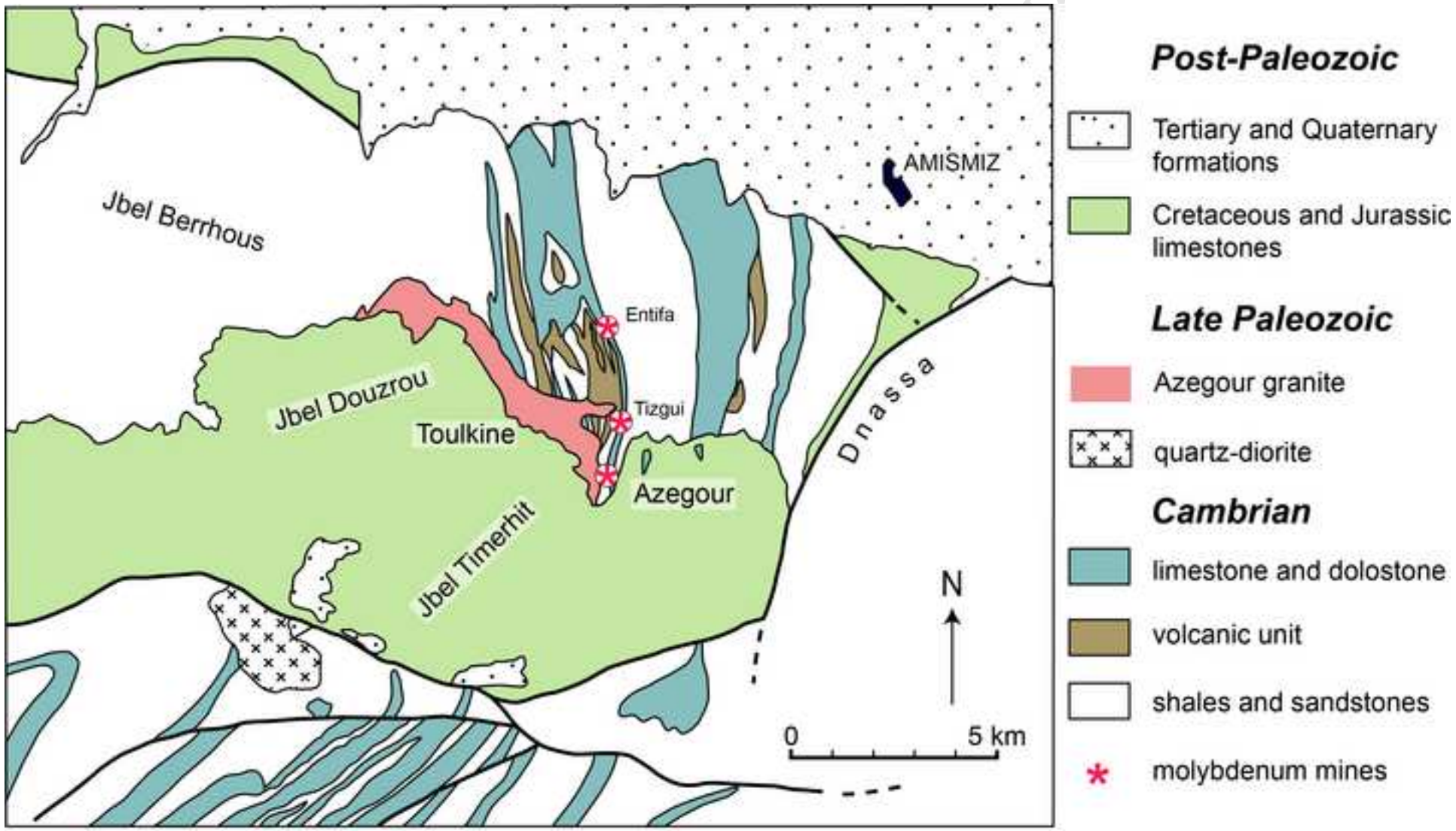
ACCEPTED MANUSCRIPT

ID	Location	Mineral
AZM 3c	Azegour mine	Chalcopyrite
AZM 3d	Azegour mine	Chalcopyrite
AZM 4a	Azegour mine	Chalcopyrite
AZM 4b	Azegour mine	Chalcopyrite
AZM5	Azegour mine	Chalcopyrite
AZM 3a	Azegour mine	Pyrrhotite
AZM 3b	Azegour mine	Pyrrhotite
AZT 1a	Tizgui road	Pyrrhotite
AZT 1b	Tizgui road	Pyrrhotite
Mo 4	Azegour mine	Molybdenite
Mo 7	Azegour mine	Molybdenite
Mo 8	Azegour mine	Molybdenite
Mo 72	Azegour mine	Molybdenite
Mo 73	Azegour mine	Molybdenite
Mo 74a	Azegour mine	Molybdenite
Mo 74b	Azegour mine	Molybdenite
Mo 74c	Azegour mine	Molybdenite
Mo 75a	Azegour mine	Molybdenite
Mo 75b	Azegour mine	Molybdenite
Mo 76a	Azegour mine	Molybdenite
Mo 76b	Azegour mine	Molybdenite
Mo 77	Tizgui mine	Molybdenite
Mo 78	Tizgui mine	Molybdenite
Mo 84a	Azegour mine	Molybdenite
Mo 84b	Azegour mine	Molybdenite
Mo 84c	Azegour mine	Molybdenite
Mo 85a	Azegour mine	Molybdenite
Mo 85b	Azegour mine	Molybdenite
Mo 85c	Azegour mine	Molybdenite
Mo 85d	Azegour mine	Molybdenite
Mo 86a	Azegour mine	Molybdenite
Mo 86b	Azegour mine	Molybdenite
Mo 87	Azegour mine	Molybdenite
Mo 88a	Azegour mine	Molybdenite
Mo 88b	Azegour mine	Molybdenite

Description			Content	
Mineral	Name	Provenance	U ppm	Th ppm
Pyrrhotite	AZT1a	Tizgui Road	0.60	0.14
	AZT1b	Tizgui Road	0.24	0.13
	AZM3a	Azegour Mine	2.57	0.09
	AZM3b	Azegour Mine	0.04	0.04
Chalcopyrite	AZM3c	Azegour Mine	0.44	0.10
	AZM3d	Azegour Mine	0.40	0.06
	AZM4a	Azegour Mine	0.05	0.03
	AZM4b	Azegour Mine	0.10	0.02
	AZM5	Azegour Mine	0.04	0.02
Molybdenite	Mo4	Azegour Mine	0.22	0.05
	Mo7	Azegour Mine	1.05	0.04
	Mo8	Azegour Mine	1.13	0.04
K-Feldspar	AZG	Azegour granite	0.81	0.53

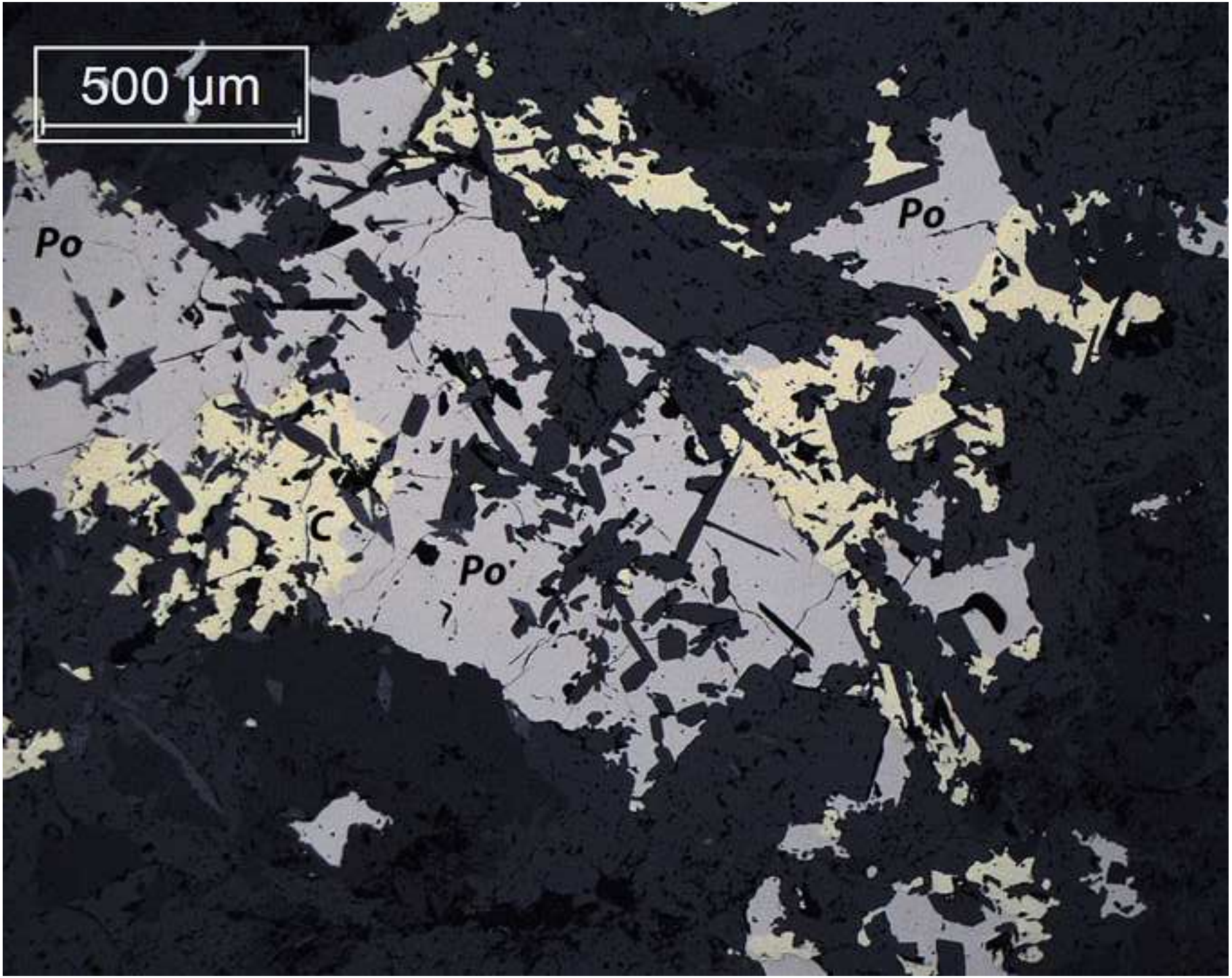
ACCEPTED MANUSCRIPT

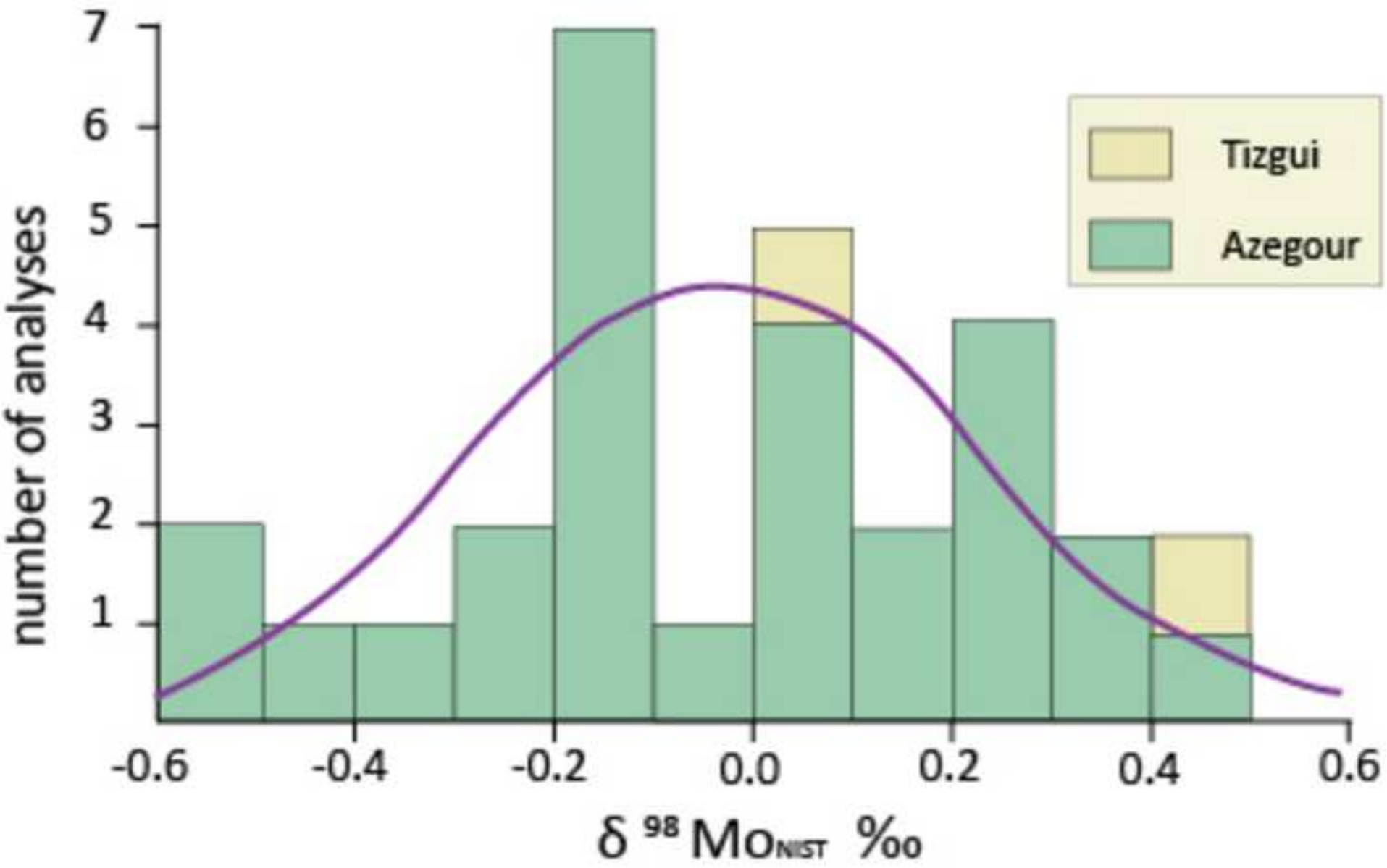

10 °W
8 °W
6 °W
4 °W
2 °W
36 °N
34 °N
32 °N
30 °N
ATLANTIC OCEAN
ALBORAN SEA
Tanger
Oujda
RIF
Fès
Rabat
Casablanca
MOROCCAN MESETA
MIDDLE ATLAS
Midelt
HIGH ATLAS
Errachidia
Marrakech
Azegour
Ouarzazate
Agadir
ANTI ATLAS
Neogen - Quaternary
Mesozoic - Paleogen
Paleozoic
Neoproterozoic granitoids (Anti Atlas)
N
200 km

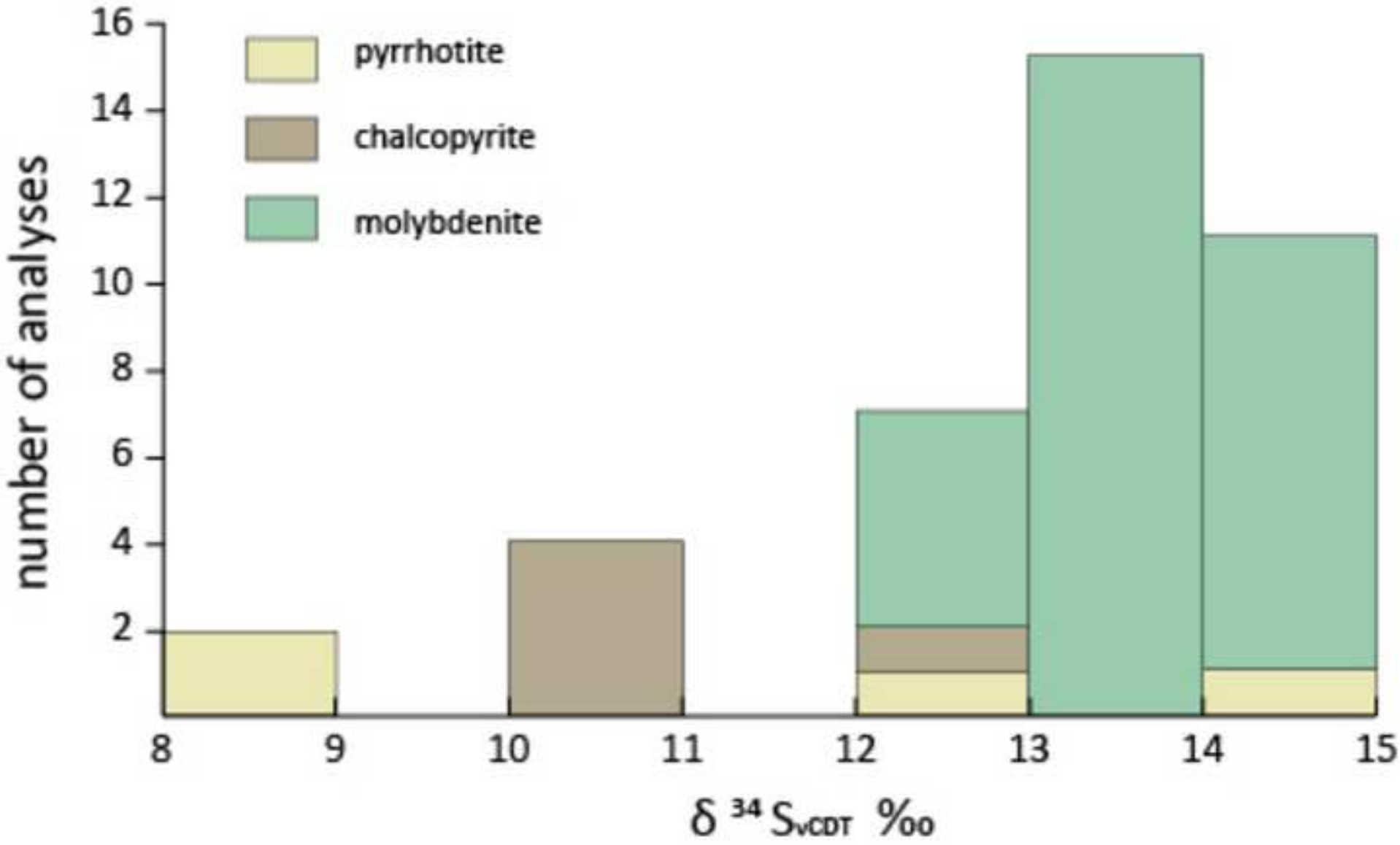

Jbel Berrhous
AMISMIZ
Entifa
Jbel Douzrou
Tizgui
Toulkine
Azegour
Jbel Timerhit
Dnassa
N
0
5 km
Post-Paleozoic
Tertiary and Quaternary formations
Cretaceous and Jurassic limestones
Late Paleozoic
Azegour granite
quartz-diorite
Cambrian
limestone and dolostone
volcanic unit
shales and sandstones
molybdenum mines

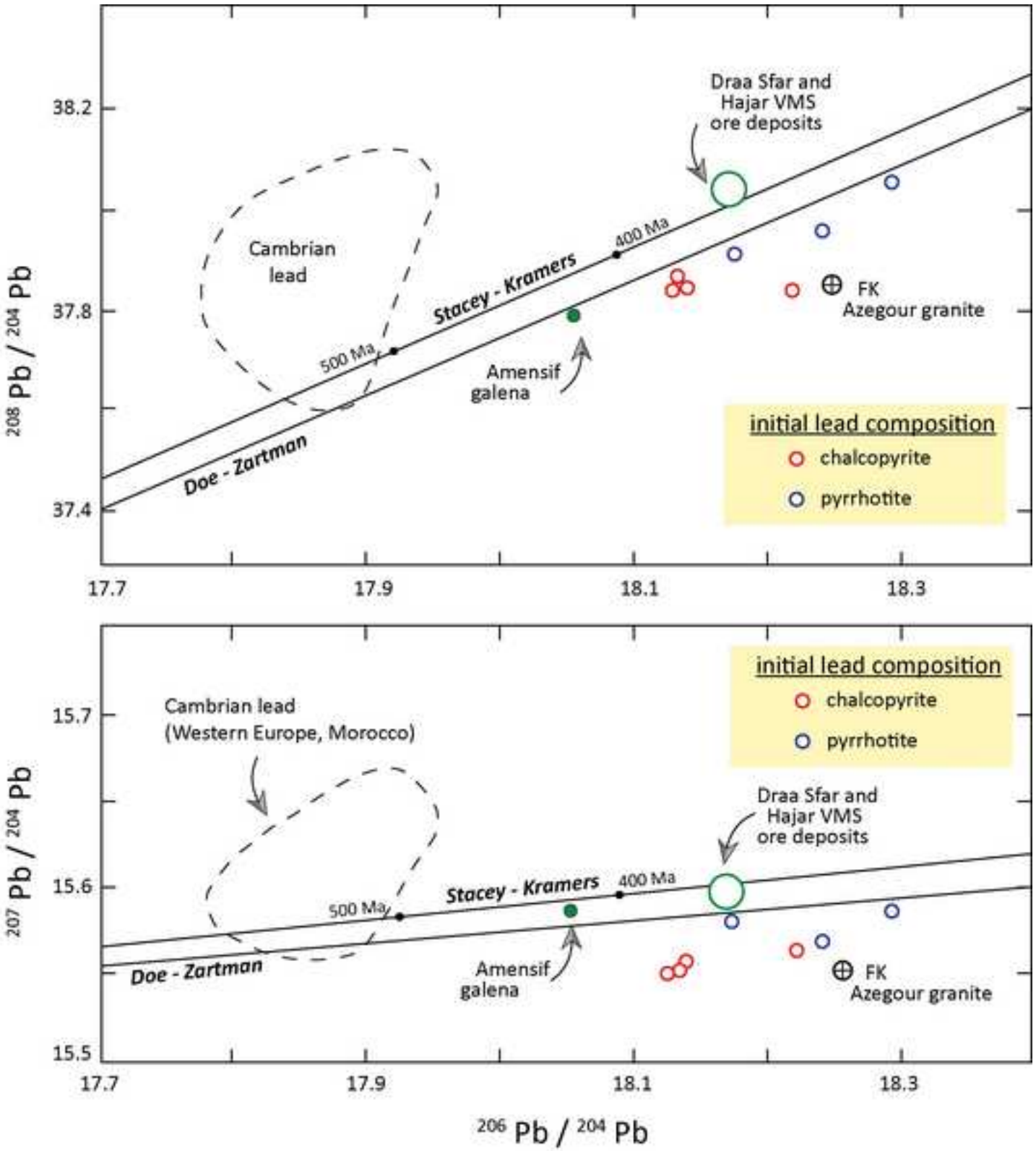

granite
skarn


500 µm


500 µm
Po
Po
C
Po


number of analyses
7
6
5
4
3
2
1
-0.6
-0.4
-0.2
0.0
0.2
0.4
0.6
δ 98 MoNIST ‰
Tizgui
Azegour


pyrrhotite
chalcopyrite
molybdenite
number of analyses
16
14
12
10
8
6
4
2
8
9
10
11
12
13
14
15
δ ³⁴ SvCDT ‰


Draa Sfar and
Hajar VMS
ore deposits
Cambrian
lead
Stacey - Kramers
400 Ma
500 Ma
Doe - Zartman
Amensif
galena
FK
Azegour granite
initial lead composition
chalcopyrite
pyrrhotite
38.2
37.8
37.4
17.7
17.9
18.1
18.3
208 Pb / 204 Pb
Cambrian lead
(Western Europe, Morocco)
15.7
15.6
15.5
207 Pb / 204 Pb
206 Pb / 204 Pb

ACCEPTED MANUSCRIPT

Highlights

- The Mo-Cu-W Azegour skarn is Permian (276 ± 1.2 Ma, Re-Os geochronology)
- Multiple Permian mineralization events associated with the Azegour granite are likely
- $\delta^{34}S$ values determined from sulphides suggest a sedimentary origin for sulphur
- Source of common lead has to be sought in the host Cambrian volcano-sedimentary units

ACCEPTED MANUSCRIPT